

# Resonant Interactions in Rotating Homogeneous Three-dimensional Turbulence

By QIAONING CHEN<sup>1</sup>, SHIYI CHEN<sup>1,2,3</sup>,  
GREGORY L. EYINK<sup>1,3</sup> AND DARRYL D. HOLM<sup>4,5</sup>

<sup>1</sup>Department of Mechanical Engineering, The Johns Hopkins University, Baltimore, MD 21218, USA

<sup>2</sup>CCSE and LTCS, Peking University, China

<sup>3</sup>Department of Applied Mathematics and Statistics, The Johns Hopkins University, Baltimore, MD 21218, USA

<sup>4</sup>Center for Nonlinear Studies and Theoretical Division, Los Alamos National Laboratory, Los Alamos, NM 87545, USA

<sup>5</sup>Mathematics Department, Imperial College London, SW7 2AZ, UK

(Received ?? and in revised form ??)

Direct numerical simulations of three-dimensional (3D) homogeneous turbulence under rapid rigid rotation are conducted to examine the predictions of resonant wave theory for both small Rossby number and large Reynolds number. The theory predicts that “slow modes” of the velocity, with zero wavenumber parallel to the rotation axis ( $k_z = 0$ ), will decouple from the remaining “fast modes” and solve an autonomous system of two-dimensional (2D) Navier-Stokes equations for the horizontal velocity components, normal to the rotation axis, and a 2D passive scalar equation for the vertical velocity component, parallel to the rotation axis. The Navier-Stokes equation for three-dimensional rotating turbulence is solved in a  $128^3$  mesh after being diagonalized via “helical decomposition” into normal modes of the Coriolis term. A force supplies constant energy input at intermediate scales. To verify the theory, we set up parallel simulations for the 2D Navier-Stokes equation and 2D passive scalar equation to compare them with the slow-mode dynamics of the 3D rotating turbulence. The simulation results reveal that there is a clear inverse energy cascade to the large scales, as predicted by 2D Navier-Stokes equations for resonant interactions of slow modes. As the rotation rate increases, the vertically-averaged horizontal velocity field from 3D Navier-Stokes converges to the velocity field from 2D Navier-Stokes, as measured by the energy in their difference field. Likewise, the vertically-averaged vertical velocity from 3D Navier-Stokes converges to a solution of the 2D passive scalar equation. The slow-mode energy spectrum approaches  $k_h^{-5/3}$ , where  $k_h$  is the horizontal wavenumber, and energy flux becomes closer to constant, as in 2D, the greater the rotation rate. Furthermore, the energy flux directly into small wave numbers in the  $k_z = 0$  plane from non-resonant interactions decreases, while fast-mode energy concentrates closer to that plane. The simulations are consistent with an increasingly dominant role of resonant triads for more rapid rotation.

## 1. Introduction

Large-scale flows in oceans and the atmosphere are greatly affected by the earth’s rotation and are known to be quasi-two-dimensional. Rotation also plays an important

role in many engineering flows, e.g. high-Reynolds turbulent flows in turbo-machinery and rotating channels. When a fluid is under rotation, the Coriolis force is introduced into the momentum equation and competes with the nonlinear force. A dimensionless number, the Rossby number  $Ro$ , may be defined as the ratio of the magnitude of the inertial term to the Coriolis force. In a rapidly rotating fluid, a mathematical limit  $Ro \rightarrow 0$  is taken of the three-dimensional Navier-Stokes equations. There is a general expectation that the fluid should become two-dimensional in this limit. For example, the classic Taylor-Proudman theorem implies that the Coriolis force will align vortex tubes parallel to the rotation axis in steady-state, rapidly-rotating flows (Greenspan (1968)).

To take into account the effect of rapid rotation on dynamical evolution a *resonant wave theory* has been applied (Greenspan (1968), Greenspan (1969), Waleffe (1993)). Similar theories were first developed for gravity waves in geophysical fluid flows (Phillips (1960)) and have since been widely invoked elsewhere. For excellent reviews, see Phillips (1981) and Craik (1985). According to this approach, the fluid velocity may be regarded in the limit of small Rossby number as a superposition of inertial waves with a large characteristic frequency which are modulated on a longer, slow time-scale. An averaged equation is derived from weakly nonlinear theory for the slow-time motion. This equation explains enhanced energy transfer from small scales to large scales by the resonant triadic interaction of inertial waves (Greenspan (1968), Greenspan (1969), Waleffe (1993)). Using an “instability hypothesis”, Waleffe (1993) argued further that resonant triadic interactions should drive the flow to become quasi-two-dimensional. More recently, this type of resonant wave theory has been put on a sounder mathematical footing. Embid & Majda (1996), Embid & Majda (1998) and Majda & Embid (1998) have derived similar “averaged equations” in a rigorous asymptotic limit over a fixed time interval for a general class of geophysical fluids problems with fast wave dynamics. For the particular case of rotating incompressible fluids, it has been shown that the averaged equations contain as a subset the 2D Navier-Stokes equations for the vertically-averaged velocity fields (Mahalov & Zhou (1996), Babin, Mahalov & Nicolaenko (1996)).

However, in *turbulent* flow under rapid rotation not only is the Rossby number  $Ro$  small, but also the Reynolds number  $Re$  is large. As a consequence, eddy motions are excited on a wide range of length scales. At any given wavenumber  $k$  there are thus at least two distinct time scales, the rotation time scale  $\tau_\Omega \sim \frac{1}{2\Omega}$  and the nonlinear time scale  $\tau_{non}(k) \sim (k^3 E(k))^{-1/2}$  (where  $E(k)$  is the energy spectrum). The validity of the wave resonance theories depend upon  $\tau_\Omega$  being shorter than all other time scales in the problem. However, for very large Reynolds numbers, there will be a range of high wavenumbers  $k$  where instead  $\tau_{non}(k) \ll \tau_\Omega$ . Thus, the resonant wave theory is likely to be valid for turbulent flows only very non-uniformly in wavenumber, if at all. The existing mathematical derivations of the theory (Embid & Majda (1996), Embid & Majda (1998), Majda & Embid (1998), Mahalov & Zhou (1996), Babin, Mahalov & Nicolaenko (1996)) are only usefully valid for low Reynolds numbers. Indeed, error fields for the resonant wave approximation are estimated in these proofs by “Sobolev norms” that get most of their contribution from high-wavenumbers. The errors are therefore shown, by present theorems, only to have upper bounds that grow rapidly with the Reynolds number  $Re$ . While the error bounds also decrease with Rossby number  $Ro$ , arguments based on comparing time-scales, like those above, suggest that resonant triads will be selected latest at the highest wavenumbers. Thus, very low Rossby numbers should be required in the existing proofs to guarantee that errors in the wave resonance theory are small for fully-developed turbulent flow.

The present evidence from simulations and experiments is also mixed as to the validity

of the theory. Simulations of decaying rotating turbulence by Bardina, Ferziger & Rogallo (1985) showed a tendency for the length-scales along the axis of rotation to grow as rotation rate increases. Bartello, M  tais & Lesieur (1994) observed two-dimensional vortices emerging from the three-dimensional flow. Hossain (1994) showed that the turbulent flow reduced to an approximate two-dimensional state and the energy cascaded to longer length scales in a  $128^3$  forced simulation. These results are roughly in accord with the wave resonance theory. The first numerical work to study explicitly the relation of flow two-dimensionalization and resonant triadic interactions was Smith & Waleffe (1999). They observed a strong two-dimensionalization and a clear inverse energy cascade. However, they suggested that non-resonant interactions might still play an important role at rotation rates achieved in their simulations. So far the detailed predictions of 2D turbulence theory have not been verified numerically in rotating 3D turbulence and the role of resonant wave interactions has remained unclear for Reynolds number  $Re \gg 1$ . Thus, it is the purpose of this paper to investigate further the limit of rapidly rotating 3D turbulence, where resonant interactions should dominate and 2D turbulence be achieved.

The remainder of this paper is organized as follows. In section 2, we review the resonant wave theory of rapidly rotating fluids, including the rigorous mathematical results. Particular attention will be paid to a ‘‘Dynamic Taylor-Proudman theorem’’ that predicts the time-evolution of the vertically-averaged or 2D fields. In Appendix A, we give an elementary derivation of this result based upon the ‘‘averaged equation’’ of the resonant wave theory. In section 3, we discuss the numerical schemes and present our simulation results to investigate the mechanism of two-dimensionalization in rotating turbulence and to study the role of resonant triadic interactions. Finally, our conclusions are presented in section 4.

## 2. Resonant Wave Theory

Rapidly rotating fluids are a multi-time scale problem. In a rotating frame of reference, the Navier-Stokes equation reads (see Greenspan (1968))

$$\partial_t \mathbf{u} + 2\boldsymbol{\Omega} \times \mathbf{u} = -\nabla P / \rho + \nu \nabla^2 \mathbf{u} - \boldsymbol{\omega} \times \mathbf{u}. \quad (2.1)$$

Here, rotation vector  $\boldsymbol{\Omega} = \Omega \hat{\mathbf{z}}$ .  $\mathbf{u}(\mathbf{x})$  is the velocity field,  $\boldsymbol{\omega} = \nabla \times \mathbf{u}$  is the vorticity field,  $\rho$  is the density,  $\nu$  is the kinematic viscosity and  $P$  is the pressure in an inertial frame modified by a centrifugal term:  $P = P_0 + \frac{1}{2}\rho\|\boldsymbol{\Omega} \times \mathbf{x}\|^2$ . If  $L$  and  $U$  are characteristic length and velocity scales, then the above equation is non-dimensionalized as

$$\partial_{\tilde{t}} \tilde{\mathbf{u}} + \frac{2}{Ro} \hat{\mathbf{z}} \times \tilde{\mathbf{u}} = -\tilde{\nabla} \tilde{P} + \frac{1}{Re} \tilde{\nabla}^2 \tilde{\mathbf{u}} - \tilde{\boldsymbol{\omega}} \times \tilde{\mathbf{u}}. \quad (2.2)$$

Here, Rossby number  $Ro$  is defined as

$$Ro = \frac{U}{\Omega L}, \quad (2.3)$$

and Reynolds number  $Re$  as

$$Re = \frac{UL}{\nu}. \quad (2.4)$$

For simplicity, we get rid of the symbol tilde from now on.

The first step in developing the resonant wave theory is to expand the governing fields into ‘‘normal modes’’, i.e. the eigenmodes of the linearized equation. In the case of rapid

rotation this corresponds to an expansion of the velocity field into *helical modes*:

$$\mathbf{u}(\mathbf{x}, t) = \sum_{\mathbf{k}} \sum_{s=\pm} a_s(\mathbf{k}, t) \mathbf{h}_s(\mathbf{k}) e^{i\mathbf{k} \cdot \mathbf{x}} \quad (2.5)$$

where  $\mathbf{h}_{\pm}(\mathbf{k})$  are defined as orthogonal eigenmodes of the curl operator, satisfying  $i\mathbf{k} \times \mathbf{h}_s = s|\mathbf{k}|\mathbf{h}_s$  with  $s = \pm 1$  (Greenspan (1968), Waleffe (1992)). In this basis, the Coriolis term is diagonalized and (2.2) can be written as

$$(\partial_t - i \frac{1}{Ro} \omega_{s_k} + \frac{1}{Re} k^2) a_{s_k} = \frac{1}{2} \sum_{\mathbf{k}+\mathbf{p}+\mathbf{q}=0} \sum_{s_p, s_q} C_{\mathbf{k}\mathbf{p}\mathbf{q}}^{s_k, s_p, s_q} a_{s_p}^* a_{s_q}^*. \quad (2.6)$$

As a convenient shorthand, we abbreviate the pair  $(\mathbf{k}, s)$  as  $s_k$ . The frequency  $\omega_{s_k} = 2s(\hat{\mathbf{z}} \cdot \mathbf{k})/k = 2sk_z/k = 2s \cos \theta_k$ , with  $\theta_k$  the angle between  $\hat{\mathbf{z}}$  and wavenumber vector  $\mathbf{k}$ . The zero frequency modes or so-called *slow modes*, with  $\omega_{s_k} = 0$ , are precisely those with  $k_z = 0$  and thus coincide with 2D modes having no variation along the rotation axis. The remaining modes with  $k_z \neq 0$  are fully 3D modes and, since they have nonzero frequency, are called *fast modes*. The slow modes can also be obtained by vertically averaging the 3D velocities  $\bar{\mathbf{u}}^{3D}(x, y) = \frac{1}{H} \int_0^H \mathbf{u}(x, y, z) dz$ , with  $H$  the vertical height of the domain.

For  $Ro \rightarrow 0$ , the solution of Eq.(2.6) is assumed in the resonant interaction theory to evolve on two distinct time-scales, the slow time  $t$  and the fast time scale  $\tau = \frac{t}{\epsilon}$  for  $\epsilon = Ro$ . A standard multiple-scale asymptotic expansion is then made with  $\partial_t \rightarrow \partial_t + \frac{1}{Ro} \partial_\tau$ . To leading order, the solution satisfies a multiple-scale Ansatz  $a_{s_k}(t, \tau) = A_{s_k}(t) e^{i\omega_{s_k} \tau}$ , consisting of inertial waves with rapid oscillations on the fast time scale and amplitude  $A_{s_k}(t)$  depending on the slow time  $t$ . This slow time-dependence is determined to eliminate secular terms growing like  $\tau$ , yielding the “averaged equation”:

$$(\partial_t + \frac{1}{Re} k^2) A_{s_k} = \frac{1}{2} \sum_{\mathbf{k}+\mathbf{p}+\mathbf{q}=0}^{\omega_{s_p}+\omega_{s_q}+\omega_{s_k}=0} \sum_{s_p, s_q} C_{\mathbf{k}\mathbf{p}\mathbf{q}}^{s_k, s_p, s_q} A_{s_p}^* A_{s_q}^*, \quad (2.7)$$

valid for a slow time  $t = O(1)$ . Only “resonant triads” satisfying

$$\omega_{s_p} + \omega_{s_q} + \omega_{s_k} = 0 \quad (2.8)$$

still remain in this equation. See Greenspan (1968), Waleffe (1993) for more details.

There are three classes of resonant triads: “fast-slow-fast” and “slow-slow-slow” and “fast-fast-fast”. We follow the convention that the first wavenumber in the triad is the one appearing on the left hand of equation (2.7), and is thus the mode which undergoes evolution due to interaction of the other two modes. For example, a “fast-slow-fast” triad gives a contribution to the evolution of a fast mode due to the interaction of another fast mode and a slow mode. In such a resonant triad, the slow mode acts simply as a catalyst for energy exchange between the two fast modes and its own energy is unchanged (Greenspan (1969), Waleffe (1993)). Formally speaking, there are resonant “slow-fast-fast” triads, but they have zero coupling coefficient. This result is known to hold more generally in the theory of resonant fluid interactions, not only for simple rotation but also for  $\beta$ -plane flows (Longuet-Higgins & Gill (1967)), stratified flows (Phillips (1968), LeLong & Riley (1991)), rotating stratified flows (Bartello (1995)), and rotating shallow-water flows (Warn (1986)). As a consequence, the slow 2D modes in the limit of rapid rotation evolve under their own autonomous dynamics. This consists of all the “slow-slow-slow” triadic interactions, each of which is resonant. The averaged equation for the autonomous 2D modes splits into two parts, as shown by Embid & Majda (1996), Babin, Mahalov & Nicolaenko (1996). As  $Ro \rightarrow 0$ , the vertically-averaged horizontal velocity

$\bar{\mathbf{u}}_H^{3D} = (\bar{\mathbf{u}}^{3D}, \bar{v}^{3D})$  satisfies the 2D N-S equation:

$$\partial_t \bar{\mathbf{u}}_H^{3D} + (\bar{\mathbf{u}}_H^{3D} \cdot \nabla) \bar{\mathbf{u}}_H^{3D} = -\nabla P_H / \rho + \nu \nabla^2 \bar{\mathbf{u}}_H^{3D}, \quad (2.9)$$

while the vertically-averaged vertical velocity  $\bar{w}^{3D}$  satisfies the 2D passive scalar equation:

$$\partial_t \bar{w}^{3D} + (\bar{\mathbf{u}}_H^{3D} \cdot \nabla) \bar{w}^{3D} = \nu \nabla^2 \bar{w}^{3D}. \quad (2.10)$$

We give an elementary (but nonrigorous) derivation of these results in the Appendix. Notice that it is not implied by this result that a flow under rapid rotation will become two-dimensional, but it does mean that the dynamics will contain an independent two-dimensional subdynamics. In this respect, the result resembles the classic Taylor-Proudman theorem for steady flows (Greenspan (1968)), so that it can be termed the ‘‘Dynamic Taylor-Proudman Theorem.’’ Precisely, the statement is that the ‘‘slow-slow-slow’’ triadic interactions yield the 2D-3C Navier-Stokes equations. 2D-3C means two variables  $(x, y)$  but three components  $(\bar{\mathbf{u}}^{3D}, \bar{v}^{3D}, \bar{w}^{3D})$ . Continuing with the accounting of resonant triads, the final set with all fast modes are called *fast-fast-fast*. The averaged equation (2.7) for the evolution of fully 3D modes contains interactions of both the ‘‘fast-slow-fast’’ and ‘‘fast-fast-fast’’ types. While these cannot transfer energy directly to slow 2D modes, Waleffe (1993) has argued that ‘‘fast-fast-fast’’ resonances do play an important role in flow two-dimensionalization. As a consequence of an ‘‘instability hypothesis’’, he has shown that energy in the fast 3D modes is transferred by this set of resonances preferentially to slower modes, with smaller (but not zero) vertical wavenumber  $k_z$ .

The multiple-scale Ansatz and the averaged equation (2.7) have been rigorously proved by Embid & Majda (1996) and Majda & Embid (1998) for a general fluid dynamical equation with fast wave dynamics, which includes rapidly-rotating fluids as a special case. The precise statement of their result is that there exists some finite time  $T > 0$  and an exponent  $p > 1 + d/2$  (with  $d$  space dimension) such that, for all  $0 < t < T$ ,

$$\sum_{\mathbf{k}, s_k} k^{2p} \left| a_{s_k}^{Ro}(t) - A_{s_k}(t) e^{i\omega_{s_k} t / Ro} \right|^2 = o(1) \quad (2.11)$$

as  $Ro \rightarrow 0$ , where  $a_{s_k}^{Ro}(t)$  is the solution of the full equation (2.6) for given Rossby number  $Ro$ , and  $A_{s_k}(t)$  is the solution of the averaged equation (2.7). Thus the error in the multiple-scale approximation goes to zero in the Sobolev-norm sense of (2.11) as  $Ro \rightarrow 0$ . This result can be stated in another way, in terms of the error field

$$\delta^{Ro}(\mathbf{x}, t) \equiv \mathbf{u}^{Ro}(\mathbf{x}, t) - \mathbf{U}(\mathbf{x}; t, Ro), \quad (2.12)$$

where  $\mathbf{u}^{Ro}(\mathbf{x}, t)$  is the solution of the rotating Navier-Stokes equation (2.2) and  $\mathbf{U}(\mathbf{x}; t, \tau)$  is the multiple-scale Ansatz written in physical space. Define  $E_\delta^{Ro}(k, t)$  as the wavenumber spectrum of the field  $\delta^{Ro}(\mathbf{x}, t)$ , or the *error energy spectrum* (Kraichnan (1970), Kraichnan & Leith (1972)). Then (2.11) is equivalent to the statement that, as  $Ro \rightarrow 0$ ,

$$\int_0^\infty dk \, k^{2p} E_\delta^{Ro}(k, t) = o(1), \quad (2.13)$$

for all  $0 < t < T$  and some  $p > 1 + d/2$ . Thus, the theorem guarantees that some moment of the error spectrum goes to zero, at least over a finite time-interval, as  $Ro \rightarrow 0$ .

The multiple-scale argument applies to any rotating 3D flow, whether laminar or turbulent. However, the error bounds in (2.11) and (2.13) assume that, for  $d = 3$ , energy spectra decay faster than  $k^{-6}$  at high wavenumbers  $k$ , much steeper than turbulent spectra in the inertial range. Of course, when the Reynolds number  $Re$  is large but finite, then the spectra shall eventually decay exponentially at large enough  $k$ , in the far dissipa-

pation range. However, because of the long inertial range, the Sobolev norms in (2.11) and (2.13) will become strongly Reynolds-number dependent, expected to grow as some power  $(Re)^{\xi_p}$ . Thus, the norms will not be small at high Reynolds number, except when the Rossby number is extremely low. Indeed, note that the spectral moments in (2.13) will get most of their contribution from near the Kolmogorov dissipation wavenumber  $k_d$  in a turbulent flow. That is the last wavenumber range where resonant triads will be selected as  $Ro \rightarrow 0$ , because the eddy turnover time  $\tau_{non}(k_d)$  in the dissipation range is the shortest in the entire flow. Therefore, the present theorems effectively say nothing about the validity of the resonant wave theory at high  $Re$ , for realistic values of the Rossby number. Since previous numerical simulations of rotating turbulence by Bardina, Ferziger & Rogallo (1985), Bartello, Mètais & Lesieur (1994), Mansour, Cambon & Speziale (1992), Hossain (1994), Smith & Waleffe (1999) have also not verified the predictions of (2.7), its status for turbulent flow has remained unclear.

### 3. Numerical Simulations and Analysis

To address this issue, we have simulated the rotating N-S equation Eq.(2.2) in a  $128^3$  periodic box with a forcing

$$f_i(\mathbf{k}, t) = \epsilon_{\mathbf{k}, i} / \hat{u}_i(\mathbf{k}, \mathbf{t})^*. \quad (3.1)$$

Here,  $\hat{u}_i(\mathbf{k}, \mathbf{t})^*$  is the conjugate of Fourier component  $\hat{u}_i(\mathbf{k}, \mathbf{t})$ . This force is specially chosen so that the energy input rates  $\epsilon_{\mathbf{k}, i}$  are all fixed (Siggia & Kerr (1978)), and we choose the latter to be constant in a narrow band  $22 < k_f < 24$  and zero elsewhere. Thus, the total input power  $\epsilon = \sum_{\mathbf{k}, i} \epsilon_{\mathbf{k}, i}$  is constant, as well as the separate energy inputs into slow modes and fast modes. This forcing guarantees also that the energy input is the same for all rotation rates. The normal viscosity term  $\nu \nabla^2 \mathbf{u}$  is replaced by a hyperviscosity term  $(-1)^{p+1} \nu_p (\nabla^2)^p \mathbf{u}$  with  $p = 8$ , to extend the inertial range. The Coriolis force and viscosity term are integrated exactly using a slaved, 2nd-order Adams-Bashforth scheme. At each time step, the velocity in Fourier space  $\hat{\mathbf{u}}(\mathbf{k}, t)$  is decomposed into the two helical modes and these two modes are evolved according to Eq.(2.6). The nonlinear term is calculated using the usual pseudospectral method and then projected onto the two helical modes (Smith & Waleffe (1999)). The macro-Rossby number  $Ro^L = (\epsilon k_f^2)^{1/3} / \Omega$  ranges from 0.066 to 0.0021. Rossby numbers from the various experimental and numerical studies are collected in Table 1. In the table *micro*- Rossby number  $Ro^\omega = \omega' / (2\Omega)$  and  $\omega'$  is *r.m.s* vorticity. Among the direct numerical simulations of forced rotating turbulence, Yeung & Zhou (1998) were interested in the dynamics in the range  $k > k_f$ , while we and others (Smith & Waleffe (1999), Hossain (1994)) focus on the dynamics in the inverse energy cascade range  $k < k_f$ . We consider a transient flow state, in which rotation is begun after a statistically steady state is reached without rotation. The results shown below, if without specification, were obtained after taking an ensemble average over eight realizations started from distinct initial conditions. This simulation is patterned after a  $128^2$  simulation of 2D N-S by Smith & Yakhot (1993). They found that an inertial-range energy spectrum  $k^{-5/3}$  is established by the 2D inverse cascade process and energy flux in the inverse cascade range is a negative constant, at least before energy begins to accumulate at the largest scales. To compare the results of our 3D rotating simulation with its hypothetical limit, described by the 2D N-S and passive scalar equations, we carry out simultaneous calculations with Eq.(2.9) and Eq.(2.10) in which the initial conditions are the vertically-averaged initial conditions of the rotating flow and the force is the vertically-averaged 3D force. In such a setup the simulation

---

Experiment/Numerical Simulations	Rossby Number	Forcing Scale
<i>Traugott</i> (1958) ( <i>decay</i> )	$Ro^\omega = 1.65$	<i>None</i>
<i>Wigeland &amp; Nagib</i> (1978) ( <i>decay</i> )	$Ro^\omega = 0.4 \sim 16$	<i>None</i>
<i>Bardina et al.</i> (1985) ( <i>decay</i> )	$Ro^\omega = 0.3 \sim 6.3$	<i>None</i>
<i>Jacquín et al.</i> (1990) ( <i>decay</i> )	$Ro^L = 0.2 \sim 12$	<i>None</i>
<i>Bartello et al.</i> (1994) ( <i>decay</i> )	$Ro^\omega = 0.01 \sim 100$	<i>None</i>
<i>Hossain</i> (1994) ( <i>forced</i> )	$Ro^L = 0.1$	$11 \leq k_f^2 \leq 13$
<i>Yeung &amp; Zhou</i> (1998) ( <i>forced</i> )	$Ro^L = 0.00064 \sim 0.0195$	$k_f \leq 2$
<i>Smith &amp; Waleffe</i> (1999) ( <i>forced</i> )	$Ro^L = 0.17, 0.35$	$k_f = 24$
<i>Our 128<sup>3</sup>DNS</i> (2003) ( <i>forced</i> )	$Ro^L = 0.0021 \sim 0.066$	$22 \leq k_f \leq 24$

---

TABLE 1. Different Rossby Numbers from Experimental and Numerical Studies

time is also the slow time. With these simulations we systematically check the main predictions of the averaged equation Eq.(2.7) for the resonant interactions.

As Rossby number asymptotically approaches zero, the resonant triadic interactions represented in the “averaged equation” should become more and more dominant over the non-resonant ones. In Table 2, all resonant and non-resonant triadic interactions and their characteristics in the rapid-rotation limit are listed. In this section, we examine carefully the validity of the resonant wave theory as we decrease the Rossby number. To be more specific, slow-slow-slow triadic interactions, slow-fast-fast triadic interactions and fast-fast-fast triadic interactions are studied, respectively. We shall not study the catalytic “fast-slow-fast” resonant triads, because these can transfer energy only between fast modes with the same wavevector magnitude  $k$  and the same value of  $\cos \theta$  (Waleffe (1993)). Hence, they can play no direct role in transferring energy between scales or in two-dimensionalization of the flow. Their plausible effect is simply to isotropize the fast mode energy distribution in the horizontal wavenumber plane.

In Fig. 1 are plotted 3D energy spectra for different Rossby numbers and also for the parallel 2D run. In the plot,  $k_h = (k_x^2 + k_y^2)^{1/2}$  is horizontal wavenumber magnitude. When rotation is “turned on”, energy is transferred to the large scales as shown in Fig. 1 (a) and (c), consistent with the previous observations (Hossain (1994) and Smith & Waleffe (1999)). Notice that large-scale energy grows faster at  $Ro = 0.066$  than at  $Ro = 0.0021$ , when the energy input is the same. For Rossby number  $Ro = 0.17$ , Smith & Waleffe (1999) observed a rapid energy transfer to low wavenumbers similar to ours at  $Ro = 0.066$ , which they interpreted as due to fast, non-resonant interactions of inertial waves. For both of our Rossby numbers, the flow tends to two-dimensionalize. In particular, Fig. 1 (b) and (d) show that slow-mode energy  $E(k_h, k_z = 0)$ , energy from vertically-averaged horizontal velocity  $E_{uv}(k_h, k_z = 0)$  and total energy  $E(k)$  all collapse together at large scales. This does not mean, however, that the fluid dynamics is that of 2D-NS. At  $Ro = 0.066$ , these three spectra are still far from the spectrum  $E_{2D}(k_h)$  of the 2D-NS solution. It is only at  $Ro = 0.0021$  that the spectra of  $k_z = 0$  nodes begin to approach the 2D-spectrum  $E_{2D}(k_h)$  suggesting that the resonant wave theory is becoming more valid for the lower Rossby number.

---

Type of triad	Resonant/Non-resonant	Characteristics as $Ro \rightarrow 0$
<i>slow – slow – slow</i>	$R$	$2D + 3C$
<i>slow – fast – fast</i>	$N$	<i>vanishing</i>
<i>fast – slow – fast</i>	$R + N$	<i>catalytic</i>
<i>fast – fast – fast</i>	$R + N$	<i>quasi – 2D</i>

---

TABLE 2. Triadic Interactions in Three-dimensional Rotating Turbulence

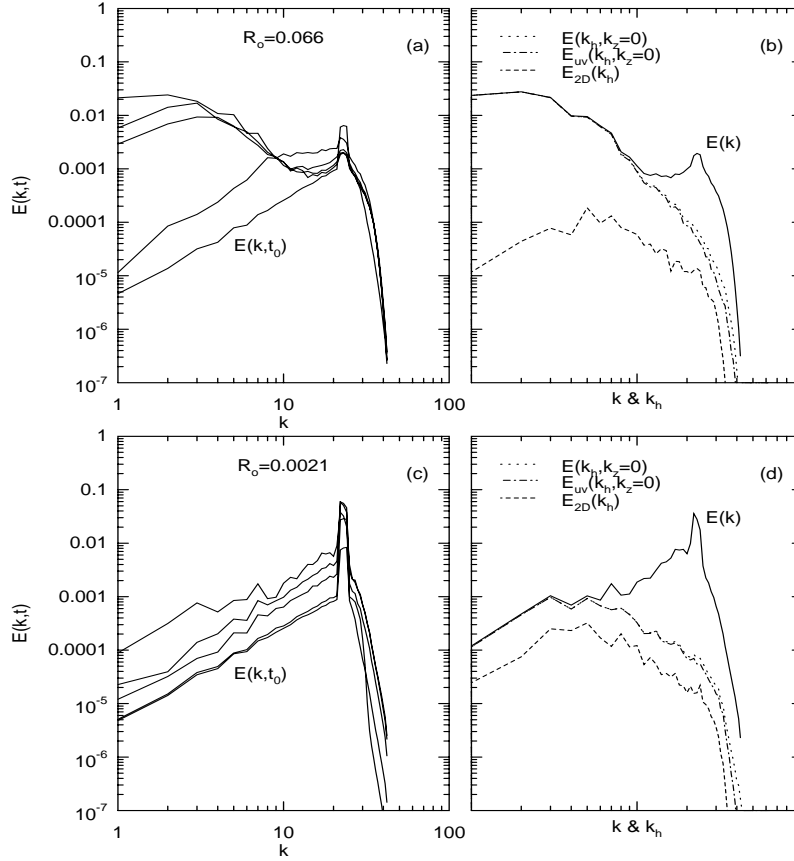


FIGURE 1. Time evolution of energy spectra (upward) for (a)  $Ro = 0.066$  and (c)  $Ro = 0.0021$  at  $t = 0$ ,  $t = 172\tau_0$ ,  $t = 344\tau_0$ ,  $t = 430\tau_0$  and  $t = 600\tau_0$ ; (b) for  $Ro = 0.066$ , large-scale motion is strongly excited and two-dimensional over a broad range of low-wavenumbers at  $t = 600\tau_0$  (from one realization) and (d) for  $Ro = 0.0021$ , large-scale motion is weaker and two-dimensional over a smaller range at  $t = 600\tau_0$  (from one realization).  $E(k, t_0)$  is the initial energy spectrum.

To investigate how energy is transferred to the large scales, we calculate the energy transfer functions  $T(k_h, k_z) = \sum_{S(k_h), I(k_z)} Re[\hat{\mathbf{u}}^* \cdot \hat{\mathbf{u}} \times \hat{\boldsymbol{\omega}}]$  at various rotation rates, where  $S(k_h)$  denotes a circular shell of horizontal wavenumbers with central radius  $k_h$  and  $I(k_z)$  is an interval of vertical wavenumbers with midpoint  $k_z$ . These energy transfer functions are plotted in Figs. 2–4, normalized by their largest absolute values. Initially before rotation is added, most of the energy transfer activity happens in the vicinity of the forcing scale  $k_f$ , where  $T(k_h, k_z)$  is negative (see Fig. 2 (a) and Fig. 3 (a)). When the system rotates slowly, at the largest simulated Rossby number  $Ro = 0.066$ , energy



is quickly carried away from the forcing scales to the  $k_z = 0$  plane and further towards smaller  $k_h$  (see Fig. 2). There is a general tendency, at all Rossby numbers, for the largest transfers at later times to be into the slow modes at  $k_z = 0$ . However, when the system rotates faster, at  $Ro = 0.00825$ , there is less energy transfer to the large scales at  $t = 450\tau_0$  (see Fig. 3). When the system rotates thirty times faster, at  $Ro = 0.0021$  (see Fig. 4), most of the energy transfer is again concentrated near the  $k_z = 0$  plane at  $t = 450\tau_0$ , but hardly any transfer has developed to smaller  $k_h$ .

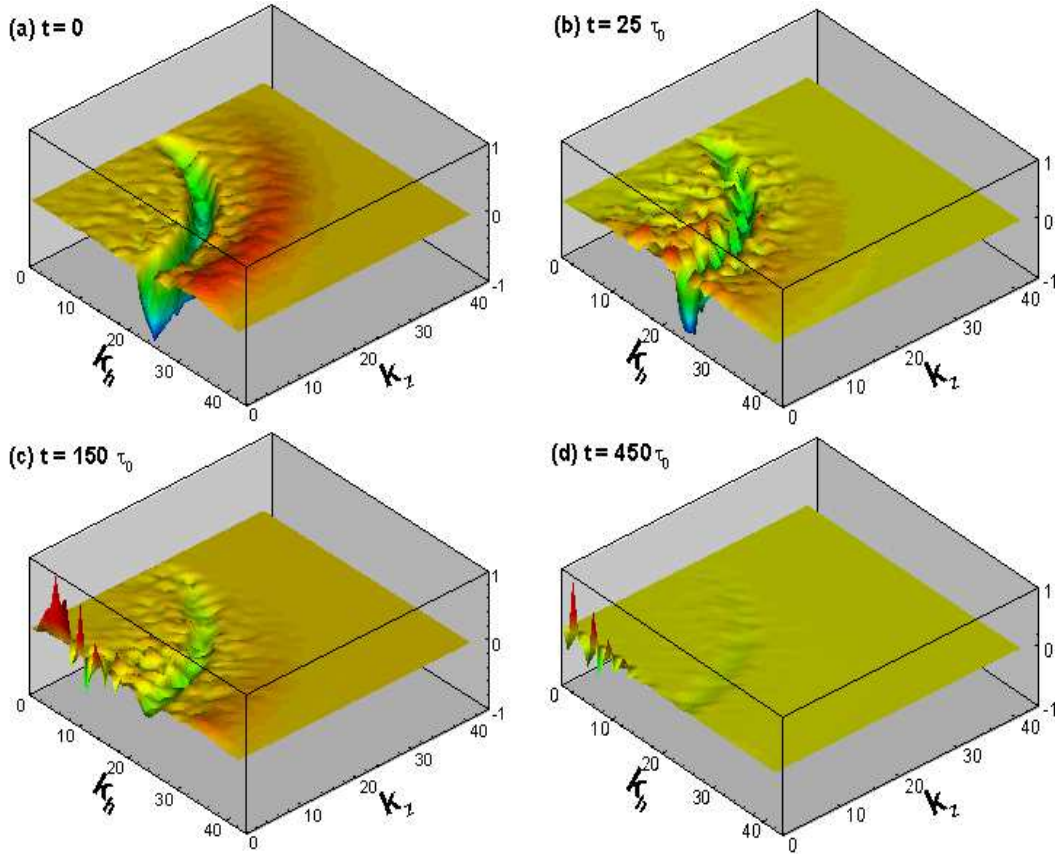


FIGURE 2. Normalized energy transfer functions  $T(k_h, k_z)/|T|_{max}$  at different times for  $Ro = 0.066$ . The red color indicates the large positive transfer and the blue color indicates the large negative transfer.

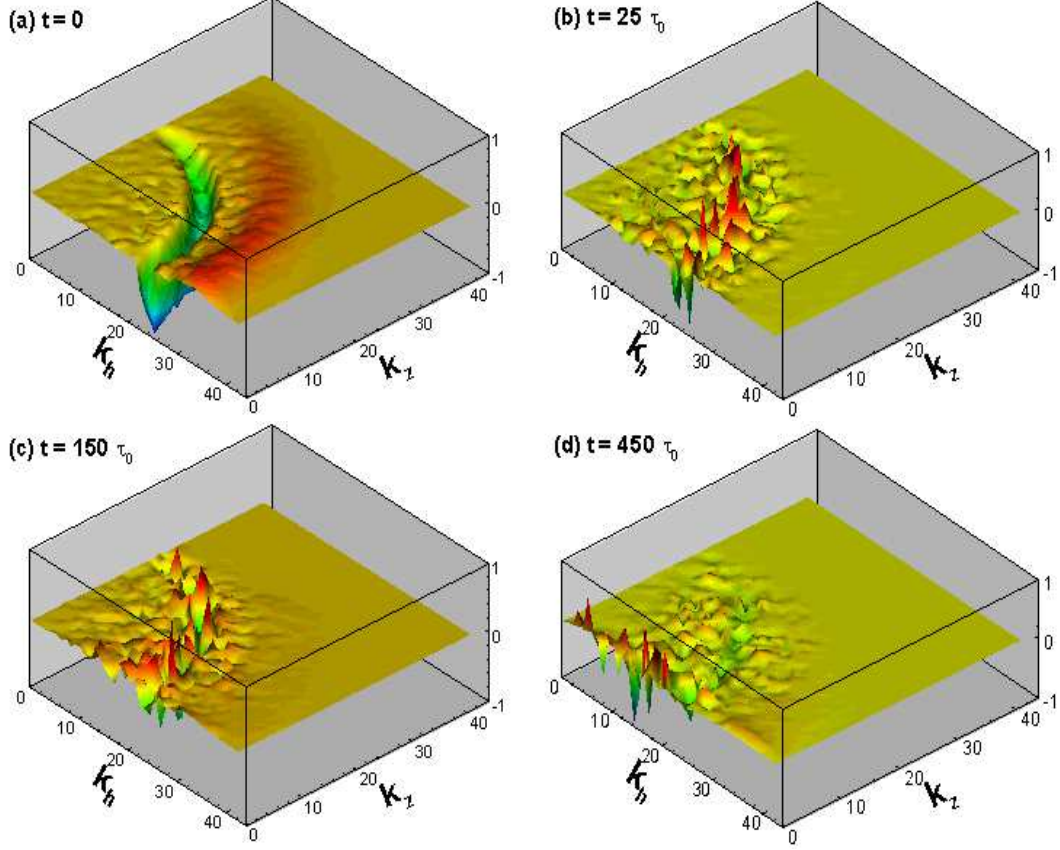
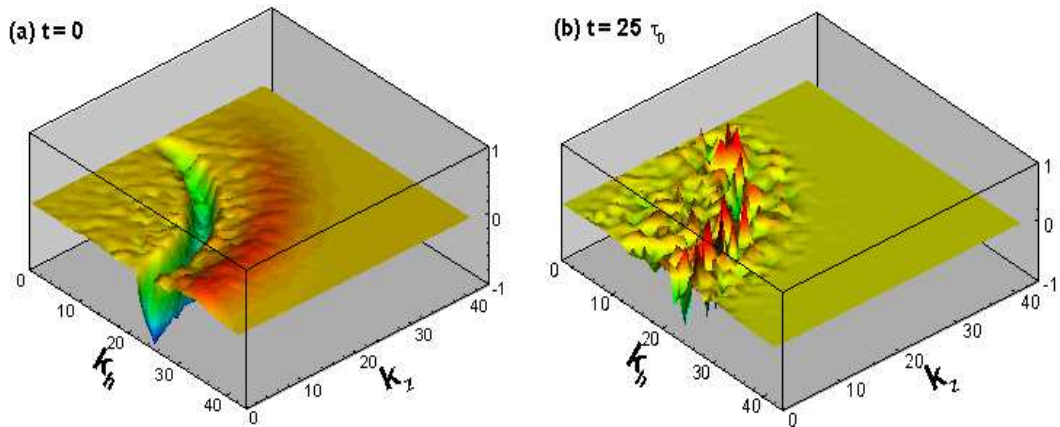


FIGURE 3. Normalized energy transfer functions  $T(k_h, k_z)/|T|_{max}$  at different times for  $Ro = 0.0085$ .



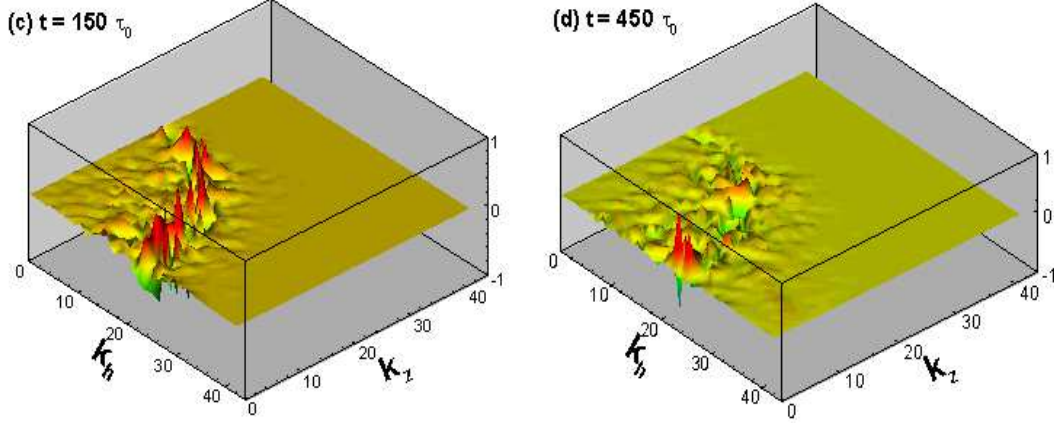


FIGURE 4. Normalized energy transfer functions  $T(k_h, k_z)/|T|_{max}$  at different times for  $Ro = 0.0021$ .

The resonant wave theory predicts not just that two-dimensionalization will occur, but also that the slow 2D modes will satisfy 2D-3C dynamics, and, in particular, should exhibit the phenomenology of the 2D inverse cascade. To test this, we study the spectral transfer at various Rossby numbers. Energy is conserved in detail for triads with all slow modes, so that we can define their energy flux  $\Pi_{sss}(k_h) = \int_{k_h}^{\infty} T_{sss}(k'_h) dk'_h$  where the energy transfer function  $T_{sss}(k_h) = \sum_{S(k_h)} Re[\hat{\mathbf{u}}^* \cdot \hat{\mathbf{u}} \times \hat{\omega}]$  only accounts for the contribution from slow modes  $k_z = 0$ .<sup>†</sup> In Fig. 5 are plotted energy fluxes  $\Pi_{sss}(k_h)$  for different Rossby numbers together with the energy flux  $\Pi_{2D}(k_h)$  from the parallel 2D simulation. At the larger Rossby number  $Ro = 0.066$ , energy fluxes not only fluctuate over time but also are much bigger than those at smaller Rossby numbers. At  $Ro = 0.0021$ , energy fluxes are negative at large scales showing a complete inverse energy cascade range. Moreover, they begin to develop a spectral range with constant value, as expected in 2D turbulence, and in fact agree closely with those from 2D-NS (Fig. 5 (c)). A consistent picture is obtained by fitting power-laws to the energy spectra, at different rotation rates. Fig. 6 (a) shows slow-mode energy spectra  $E(k_h, k_z = 0)$  are closer to  $k^{-3}$  than  $k^{-5/3}$  at  $Ro = 0.066$ , in agreement with the findings of Smith & Waleffe (1999) at comparable Rossby numbers. However, at  $Ro = 0.0021$  the spectrum scales as  $k^{-5/3}$  (Fig. 6 (b)) similar to that of the parallel 2D-NS simulation in Fig. 6 (c) and as expected for a transient 2D inverse cascade with this forcing (Smith & Yakhot (1993)).

<sup>†</sup> Before we calculate the transfer function  $T_{sss}(k_h)$ , we need to zero out the velocity field for the fast modes  $k_z \neq 0$ .

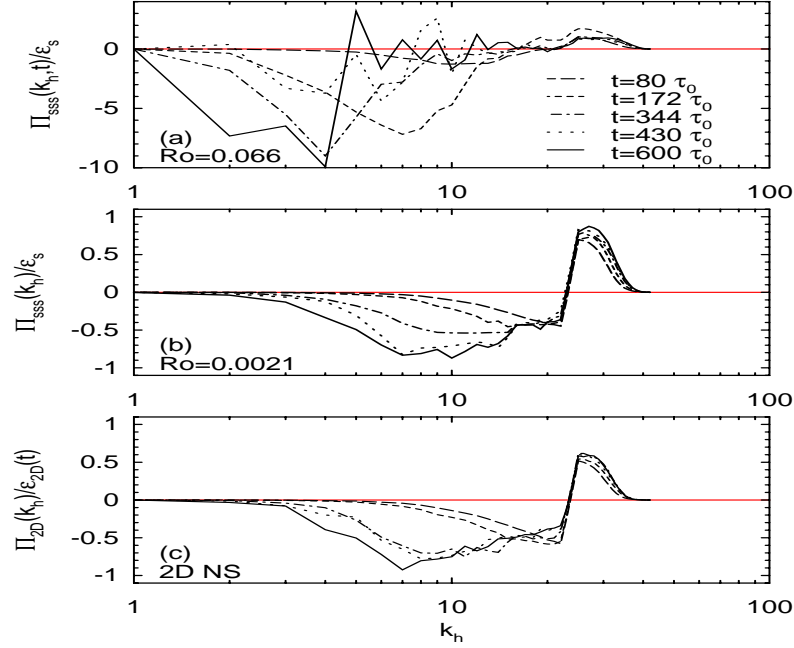


FIGURE 5. Normalized energy fluxes from *slow-slow-slow* interactions for (a)  $Ro = 0.066$ ; (b)  $Ro = 0.0021$ ; (c) normalized energy flux from 2D Navier-Stokes at different times. Here,  $\epsilon_s$  is slow-mode energy input for 3D-NS with rotation and  $\epsilon_{2D}(t)$  is energy input for 2D-NS;  $\tau_0$  is the initial large eddy turnover time.  $\epsilon_s$  is the same for every rotation rate in our study.

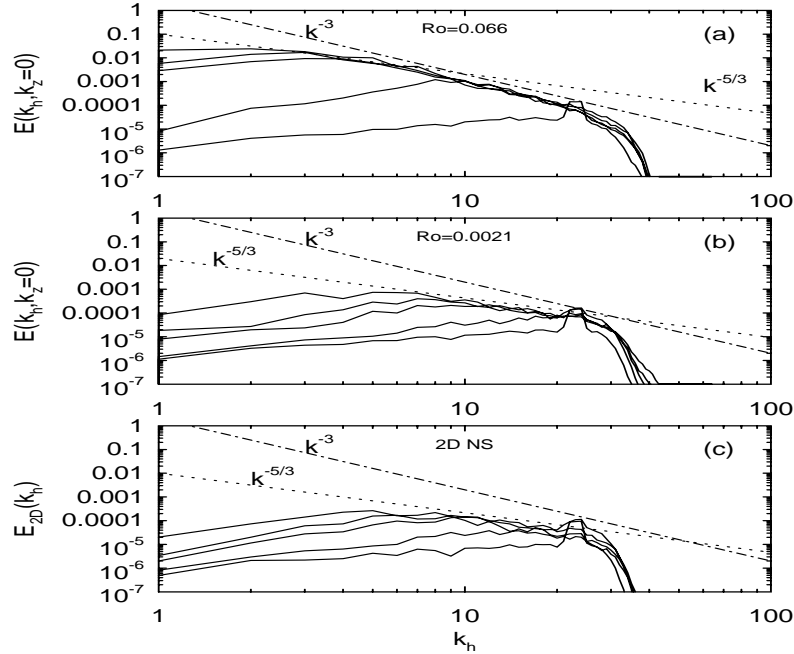


FIGURE 6. Time evolution of energy spectra (upward) from (a) slow modes at  $Ro = 0.066$ ; (b) slow modes at  $Ro = 0.0021$ ; (c) 2D-NS at  $t = 80\tau_0$ ,  $t = 172\tau_0$ ,  $t = 344\tau_0$ ,  $t = 430\tau_0$  and  $t = 600\tau_0$ .

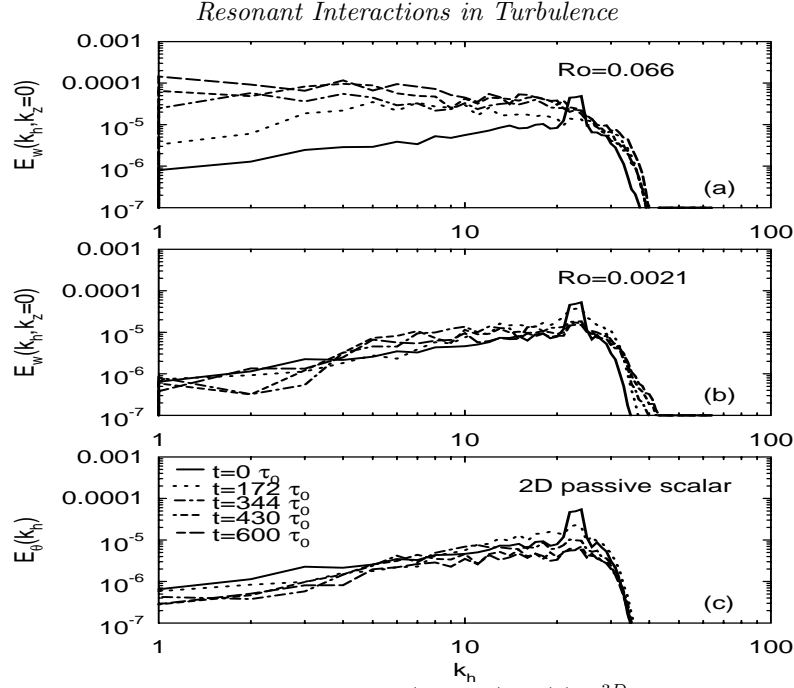


FIGURE 7. Time evolution of energy spectra (upward) of (a)  $\bar{w}^{3D}$  at  $Ro = 0.066$ ; (b)  $\bar{w}^{3D}$  at  $Ro = 0.0021$  and (c) 2D passive scalar  $\theta^{2D}$ .

In Fig. 7 we present at various Rossby numbers the time evolution of the energy spectrum  $E_w(k_h, k_z = 0)$  of the vertically-averaged vertical velocity  $\bar{w}^{3D}$ , compared with the time evolution of the spectrum  $E_\theta(k_h)$  of a passive scalar in the 2D parallel simulation. Fig. 7(a) shows that at the highest simulated Rossby number  $Ro = 0.066$  there is a tendency for an inverse cascade of  $\bar{w}^{3D}$  towards the large scales. This is opposite to what happens for a passive scalar in a 2D inverse energy cascade range, which is well known to experience a direct cascade to high wavenumber: see Celani et al. (2000) and our own Fig. 7 (c). However, as  $Ro$  decreases, the energy spectra of  $\bar{w}^{3D}$  become closer to those of the 2D passive scalar, especially at the lowest simulated Rossby number  $Ro = 0.0021$  (see Fig. 7 (b)). Thus,  $\bar{w}^{3D}$  tends also to transfer downscale as the rotation rate increases.

The difference between the 3D slow-mode dynamics and 2D-NS at finite Rossby numbers is also reflected in their different flow structures. In Figs. 8–10 are plotted the iso-surfaces of the vertically-averaged vertical vorticity  $\bar{\omega}_z^{3D}$  from the 3D flow and those of the 2D vorticity  $\omega^{2D}$ . Here, the averaged vertical vorticity is  $\bar{\omega}_z^{3D} = \frac{1}{H} \int_0^H \omega_z(x, y, z) dz$ . In Fig. 8 the formation of large vortices is seen at the higher Rossby number  $Ro = 0.066$ . Both cyclonic and anticyclonic vortices are present in the flow, which is different from the observations from Smith & Waleffe (1999). In their simulations, only cyclonic vortices were observed at larger Rossby numbers. At the same time, large vortices are not visible in the 2D turbulent flow, which seems still in its infancy (see Fig. 10). However, at a much smaller Rossby number  $Ro = 0.0021$ , the flow structures in 3D bear a strong resemblance to those seen in 2D (see Fig. 9 and Fig. 10).

The Dynamic Taylor-Proudman Theorem predicts that the 3D slow modes will obey the 2D-3C Navier-Stokes equations, asymptotically for low Rossby numbers. As we discussed in the previous section, Embid & Majda (1996) and Majda & Embid (1998) measured the size of the deviations from this prediction by Sobolev norms of the error field with large  $p$ , which do not yield useful estimates for high Reynolds number flow. Therefore, we shall consider here instead  $p = 0$ , or the error energy itself, as in Kraichnan

(1970) and Kraichnan & Leith (1972). It is useful to divide this error energy into separate contributions from horizontal and vertical velocity components. Precisely, we define

$$E_{\delta,H}(t) = \frac{1}{2} \int d^2\mathbf{x} |\bar{\mathbf{u}}_H^{3D} - \mathbf{u}^{2D}|^2, \quad E_{\delta,V}(t) = \frac{1}{2} \int d^2\mathbf{x} |\bar{w}^{3D} - \theta^{2D}|^2. \quad (3.2)$$

As before,  $\bar{\mathbf{u}}_H^{3D} = (\bar{u}^{3D}, \bar{v}^{3D})$  and  $\bar{w}^{3D}$  are the vertically-averaged horizontal and vertical velocities, respectively. For comparison,  $\mathbf{u}^{2D} = (u^{2D}, v^{2D})$  is the solution of the 2D-NS equation (2.9) and  $\theta^{2D}$  is the solution of the 2D passive scalar equation (2.10). In Fig. 11 (a) and (b) are shown the error energies in (3.2), normalized by the energies  $E_H(t, Ro)$ ,  $E_V(t, Ro)$  of the corresponding 3D vertically-averaged fields, as functions of time at different Rossby numbers. Both plots show that the normalized error energy, at least over a finite interval of time, decreases as Rossby number is lowered. For any finite value of  $Ro$ , the vertically-averaged 3D solutions and the 2D solutions begin to diverge as time  $t$  increases because of their chaotic dynamics and become uncorrelated, leading to saturation of the normalized error energy at sufficiently long times. Although presently available theorems do not rigorously imply the behavior observed in Fig. 10 for the  $p = 0$  norms, nevertheless these results are quite in line with expectations from the formal multi-time scale analysis (Greenspan (1968), Waleffe (1993)).

An important quantity to determine is the maximal length  $T_*$  of the slow-time interval over which the resonant wave theory becomes valid as  $Ro \rightarrow 0$ . The rigorous theorems guarantee that a finite time  $T > 0$  exists so that Sobolev norms of the error (with  $p > 1+d/2$ ) converge to zero for all slow times  $t \in [0, T]$ . However, the asymptotic analysis does not determine the largest possible time  $T$  for which this is true. In order to estimate this, we have defined  $T(Ro)$  for each Rossby number  $Ro$  as the time  $t$  for which the normalized error energy plotted in Fig. 10(a) first reaches the value 0.5. This quantity is plotted as a function of  $Ro$  in Fig. 12. For a wide range of Rossby numbers above 0.00825, the graph can be fit by a power-law  $Ro^{-1/2}$  with a small error bar (only 2%). The reason for such a power law to exist in this range is not clear. Interestingly, there appears to exist a transition when Rossby number is below 0.00825 and the graph tends to saturate to a constant. If true, this implies that the resonant wave theory can be valid, even for arbitrarily small  $Ro$ , only in a finite time interval of length  $< T_* = \lim_{Ro \rightarrow 0} T(Ro)$ .



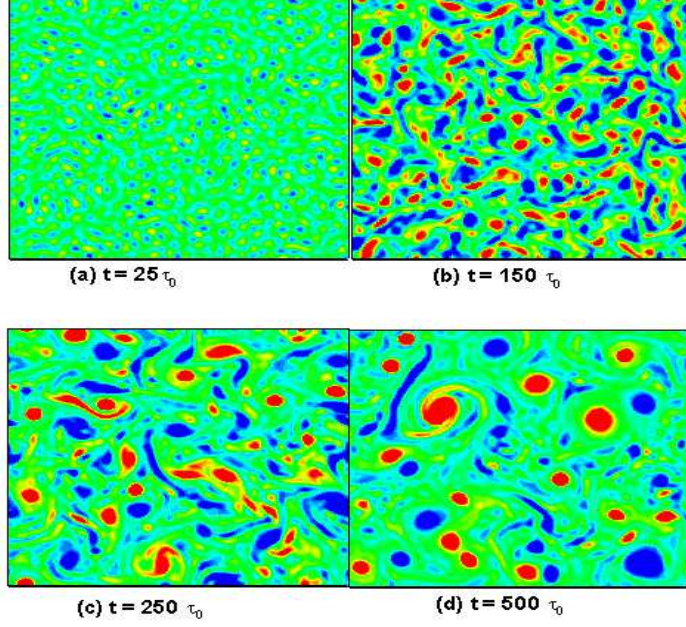


FIGURE 8. Time histories of the vertically-averaged vertical vorticity  $\overline{\omega}_z^{3D}$  iso-surfaces from 3D rotating turbulence at  $Ro = 0.066$ . The red color is for the large positive vorticity and the blue one is for the large negative vorticity.

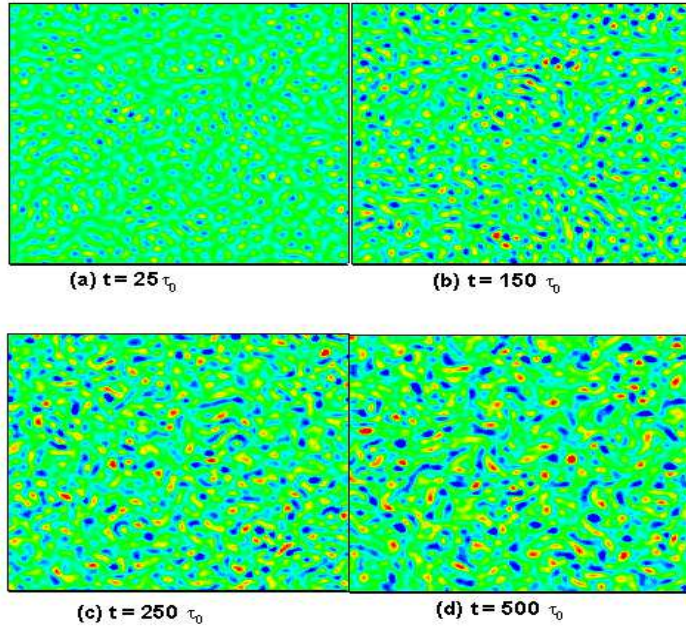
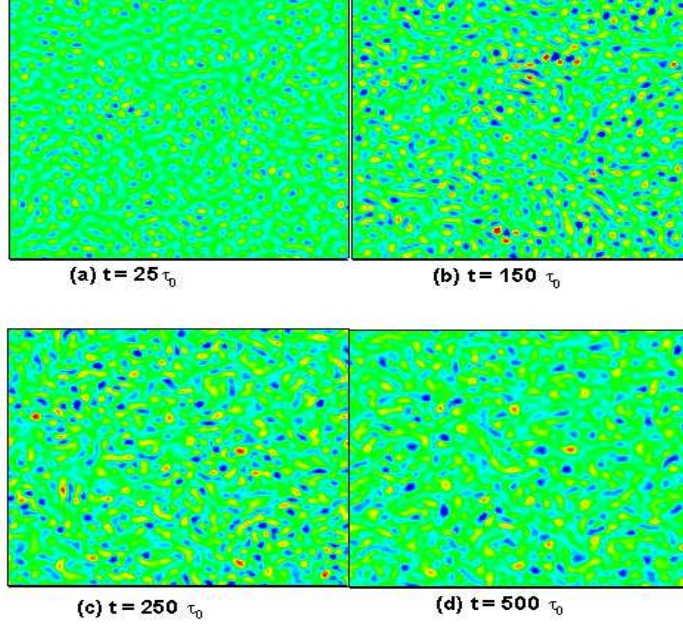
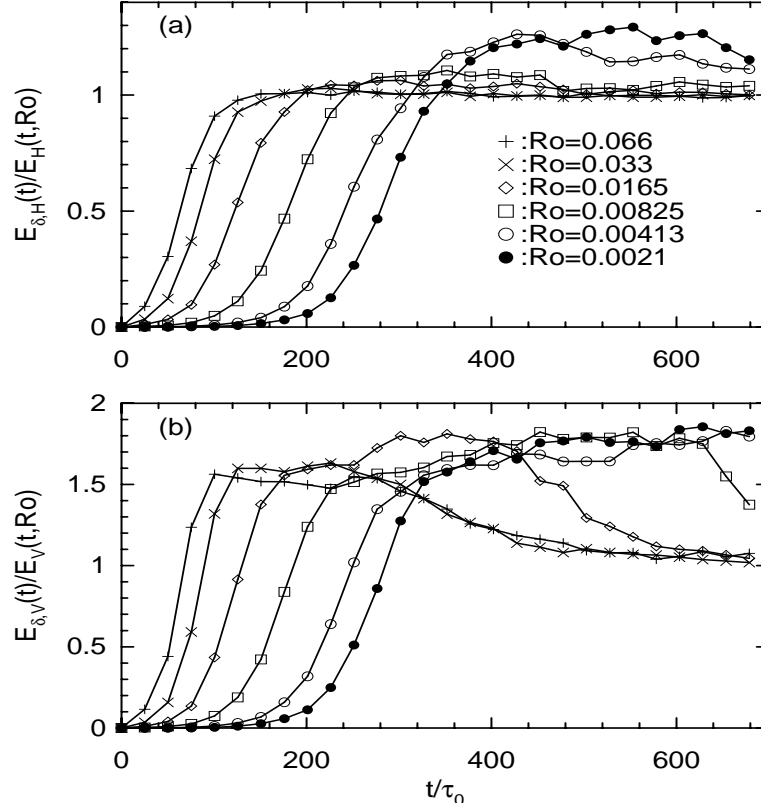
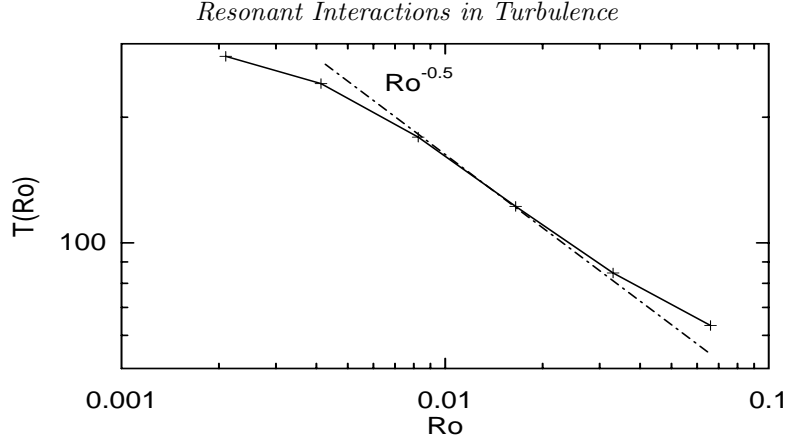


FIGURE 9. Time histories of the vertically-averaged vertical vorticity  $\overline{\omega}_z^{3D}$  iso-surfaces from 3D rotating turbulence at  $Ro = 0.0021$ .

FIGURE 10. Time histories of the  $\omega_z^{2D}$  vorticity iso-surfaces from 2D-NS.FIGURE 11. Normalized error energy for (a)  $\bar{\mathbf{u}}_H^{3D} - \mathbf{u}^{2D}$  and (b)  $\bar{\mathbf{w}}^{3D} - \theta^{2D}$ , as functions of time at different Rossby numbers. Here  $E_H(t, Ro) = \frac{1}{2} \int |\bar{\mathbf{u}}_H^{3D}|^2$  and  $E_V(t, Ro) = \frac{1}{2} \int |\bar{\mathbf{w}}^{3D}|^2$ .





17

FIGURE 12. Time  $T(Ro)$  vs. Rossby number  $Ro$ . There exists a power law scaling  $Ro^{-0.5}$  in the range  $Ro > 0.00825$  but the graph appears possibly to plateau below  $Ro = 0.00825$ .

These findings are consistent with the expected segregation of the autonomous 2D slow modes from the 3D fast modes at low Rossby numbers. All “slow-fast-fast” triads transferring energy from a slow mode by interactions with two fast modes are non-resonant and it is another main prediction of the resonant wave theory that such transfer should disappear as  $Ro \rightarrow 0$ . To test this, we calculate an energy flux into low-wavenumber slow modes from slow-fast-fast triadic interactions. Precisely, we define  $\Pi_{sff}(k_h) = -\int_0^{k_h} T_{sff}(k', k_z = 0) dk'$  where  $T_{sff}(k_h, k_z = 0) = T(k_h, k_z = 0) - T_{sss}(k_h)$  is the energy transfer function from fast modes into slow modes at horizontal wavenumber  $k_h$ . Fig. 13 (a-c) show that energy flux into slow modes at small  $k_h$  decreases as  $Ro$  decreases. In another words, less and less fast-mode energy is transferred into the large scales in the 2D plane as  $Ro \rightarrow 0$ . At larger Rossby numbers, more energy is drained from fast modes directly into the large-scale slow modes by such non-resonant transfer, causing the flow to become two-dimensional more quickly than at smaller Rossby numbers. Smith & Waleffe (1999) suggested that this non-resonant mechanism was responsible for the rapid two-dimensionalization in their simulation at larger Rossby numbers. †

† Although we agree with their conclusion, we do not find the argument they offered very convincing. In their simulation, the forcing was white-noise in time with a wavenumber spectrum  $F(k) = \epsilon_k \exp(-0.5(k - k_f)^2/\sigma^2)/\sqrt{2\pi\sigma^2}$ , nonzero in a spherical shell with mean radius  $k_f$  and width  $\sigma$ . They attributed the strong two-dimensionalization they observed to non-resonant interactions, because of what they claimed was purely three-dimensional forcing. However, their forcing input energy not only into the fully three-dimensional modes but also into two-dimensional modes in the circular band where the spherical shell intersects the  $k_z = 0$  plane. This energy will inverse cascade to large scales by “slow-slow-slow” resonant interactions.

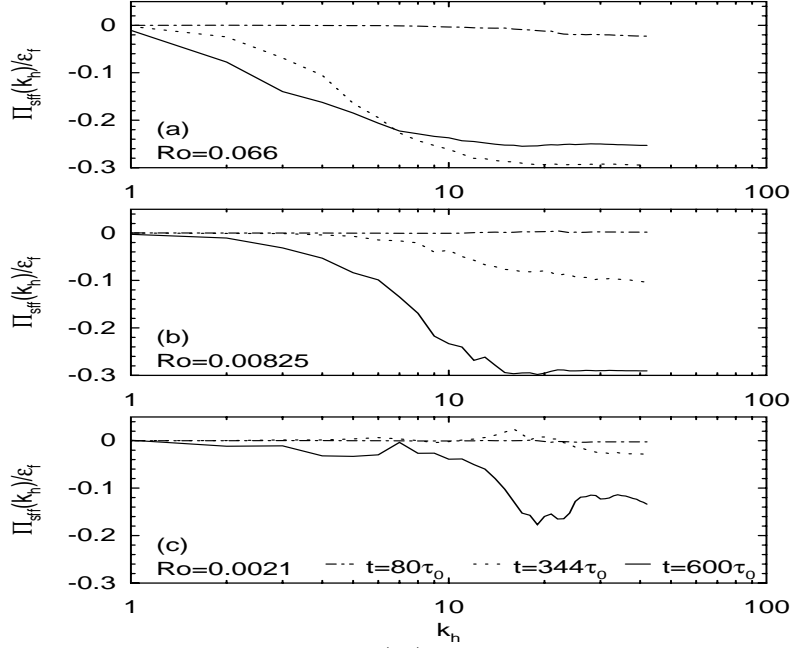
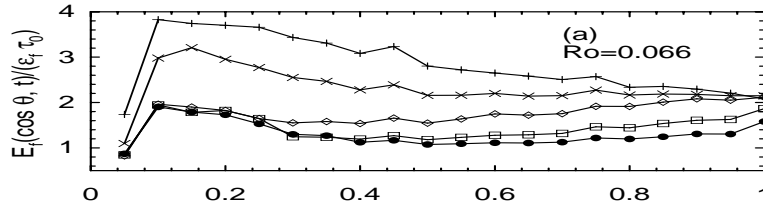


FIGURE 13. Normalized energy fluxes  $\Pi_{sff}(k_h)$  from slow-fast-fast interactions for (a)  $Ro = 0.066$ ; (b)  $Ro = 0.00825$ ; (c)  $Ro = 0.0021$  at different times. Here,  $\epsilon_f$  is the total energy input into the fast 3D modes.

A final prediction of the resonant wave theory is that, as  $Ro \rightarrow 0$ , fast-mode energy will tend to be transferred toward smaller values of  $\cos \theta$  by “fast-fast-fast” resonant interactions. Waleffe (1993) has demonstrated this tendency using the resonance condition (2.8) and a plausible “instability hypothesis,” which asserts that energy will tend to be transferred out from the unstable leg of a wavevector triad. Mansour, Cambon & Speziale (1992) and Cambon & Jacquin (1989) have observed that energy was transferred towards small  $\cos \theta$ . However, neither distinguished fast-modes from slow-modes. Thus, the effects they saw may also be due to non-resonant transfer from fast modes directly into slow-modes. In order to investigate the “fast-fast-fast” interactions, we calculate the energy distribution  $E_f(\cos \theta, t)$  only from fast modes. (We recall that the catalytic “fast-slow-fast” interactions can only transfer energy between fast modes with the same value of  $\cos \theta$  and thus cannot contribute to the dynamics of this quantity.) Fig. 14 (a) shows that  $E_f(\cos \theta, t)$  flattens monotonically with time at the largest Rossby number  $Ro = 0.066$ , implying fast modes behave largely as three-dimensional. At the middle Rossby number  $Ro = 0.00825$  (Fig. 14 (b)),  $E_f(\cos \theta, t)$  peaks at smaller  $\cos \theta$  at earlier times and then flattens everywhere at later times. However, at the smallest Rossby number  $Ro = 0.0021$ , fast-mode energy monotonically builds up at small  $\cos \theta$  (Fig. 14 (c)). This supports the conclusions of Waleffe (1993) based on the “instability hypothesis”.



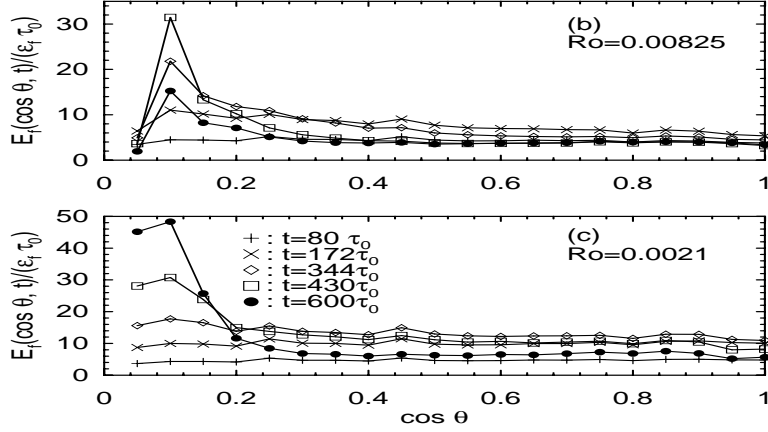


FIGURE 14. Normalized fast-mode energy distributions  $E_f(\cos\theta, t)/(\epsilon_f\tau_0)$  for (a)  $Ro = 0.066$ ; (b)  $Ro = 0.00825$ ; (c)  $Ro = 0.0021$  at different times.

#### 4. Conclusions

To summarize briefly our results, this is the first numerical simulation of forced homogeneous rotating turbulence to explore quantitatively the long-time effects of resonant interactions on the two-dimensionalization as  $Ro \rightarrow 0$ . We demonstrate an inverse cascade regime with the characteristics of 2D turbulence, namely, a  $k_h^{-5/3}$  spectral range where energy flux is negative and constant for the slow-mode dynamics. This is consistent with the predictions of 2D-3C equations, corresponding to resonant interactions. Three additional findings verify the increasing importance of resonant interactions to two-dimensionalization at small  $Ro$ . First, vertically-averaged 3D velocities ( $\bar{u}^{3D}, \bar{v}^{3D}, \bar{w}^{3D}$ ) and the solutions of 2D-3C equations converge as  $Ro \rightarrow 0$ , in the sense that the energy in their difference fields vanishes. Second, non-resonant energy flux into small  $k_h$  in the  $k_z = 0$  plane from slow-fast-fast triads decreases as  $Ro$  decreases. Finally, fast-mode energy is transferred toward the  $k_z = 0$  plane, consistent with the prediction of Waleffe (1993) that resonant interactions of fast modes drive the flow to become quasi-2D.

Our work has investigated rapidly-rotating turbulent fluids as a case study in the application of resonant wave theory. The results of the study therefore have more general interest than for this particular problem. The same type of theory has been widely applied to geophysical turbulent flows with rotation and/or stratification (Phillips (1981), Craik (1985)). Details of the predictions may differ considerably according to the context. For example, Bartello (1995) used a similar reasoning as that of Waleffe (1993) to argue that for rotating, stratified turbulence the catalytic, “fast-slow-fast” resonant triads will transfer the energy in fast gravity waves downscale and provide a primary mechanism of nonlinear geostrophic adjustment, while the “fast-fast-fast” resonant interactions will be of secondary importance. In rapidly rotating fluids without density stratification, we find that the opposite is true. Nevertheless, many of the basic issues are the same in all applications of the resonant wave theory to high Reynolds-number turbulent flows. Therefore, it may be useful to summarize several key conclusions from our investigation of this one example.

First, the main predictions of the wave-resonance theory appear to hold for  $Ro \ll 1$  and  $Re \gg 1$  simultaneously. Convergence of the approximation holds in the useful sense that the energy in the error fields decreases to zero, over a finite time-interval. Present rigorous

theorems (Embid & Majda (1996), Embid & Majda (1998), Majda & Embid (1998)) use Sobolev-norm estimates that yield useful estimates for rotating laminar flows, but not for fully-developed turbulence. An optimistic conclusion of our work is that those theorems can probably be improved, by substitution of an  $L^2$  or energy norm for the Sobolev norms. A proof of this may not be easy, given the current lack of understanding of the inviscid, high-Reynolds number limit of fluid equations. However, our numerical results lend support to the idea that the energy-containing, large-scale motions in turbulent flow will conform to the predictions of resonant wave theory in the appropriate limit.

We find that there is an intrinsic time restriction on the validity of the resonant wave theory. The formal multiple-scale analysis, as well as the rigorous theorems, predict that there should be a finite interval of the slow-time variable  $t$  over which the approximation will converge. They do not answer the question whether this time-interval is finite in fact, or whether the approximation will be valid at any arbitrary time for a sufficiently small Rossby number. Our numerical results seem to indicate either that the convergence holds over only a finite time-interval or else that the Rossby numbers required for a close approximation become extremely small beyond a certain time-horizon. Of course, both the dynamics involved—rotating 3D-NS (2.2) and the low Rossby-number limiting dynamics given by the averaged equation (2.7)—are chaotic at high Reynolds number and a rapid exponential divergence of their solutions is to be expected for finite  $Ro$ . This does not imply a necessary failure of the resonant wave theory applied to forced, statistically stationary turbulence, since chaotic dynamics often possess “structural stability” of their long-time statistics.

A more serious limitation of the wave-resonance theory may be the magnitude of the Rossby numbers required for convergence, even at relatively early times. We have found sizable non-resonant effects for Rossby numbers as small as  $Ro = 0.066$ . Since the Rossby number is not extremely small in most engineering applications, flow two-dimensionalization is there probably due mainly to the non-resonant interactions, for which the 2D dynamics is not segregated from the 3D dynamics. However, the resonant wave theory provides the correct “rapid-distortion limit” for fast rotations. Therefore, it may still be useful to take into account the resonance conditions in statistical modeling schemes for engineering purposes, as a constraint which becomes exact as  $Ro \rightarrow 0$ . Resonant interactions may be more important for geophysical flows, where typical Rossby numbers are much smaller. However, for the atmosphere at midlatitude synoptic-scales, the typical Rossby number is only about  $Ro = 0.1$  and even for the Gulf Stream with smaller characteristic velocities the Rossby number is only  $Ro = 0.07$  (Pedlosky (1987)). In our simulations, this is a marginal value to observe the predictions of the theory. A combination of rotation with other effects such as stratification may be necessary in the atmosphere and oceans to select resonant interactions of fast waves.

**Acknowledgements.** Direct numerical simulations are performed in LSSC-II at the State Key Laboratory on Scientific and Engineering Computing in China and at the cluster computer supported by NSF Grant No. CTS-0079674 at the Johns Hopkins University.

## Appendix A. Dynamic Taylor-Proudman Theorem

Here, we use the helical decomposition to give a simpler and self-contained derivation of the Dynamic Taylor-Proudman Theorem for the “slow-slow-slow” resonant triadic interactions. In a triad consisting of all slow modes  $\mathbf{k}, \mathbf{p}$  and  $\mathbf{q}$ , then  $k_z = 0$ ,  $p_z = 0$  and

$q_z = 0$ . In the  $k_z = 0$  plane or 2D plane, the wave number vector  $\mathbf{k} = k_x \hat{\mathbf{x}} + k_y \hat{\mathbf{y}}$  and its amplitude  $k = \sqrt{k_x^2 + k_y^2}$ . By choosing the helical modes  $\mathbf{h}_s(\mathbf{k}) = \mathbf{N} \times \hat{\mathbf{k}} + is\nu$  which satisfy  $i\mathbf{k} \times \mathbf{h}_\pm = \pm |\mathbf{k}| \mathbf{h}_\pm$  (Waleffe (1992)), we have

$$\mathbf{h}_s(\mathbf{k}) = \hat{\mathbf{z}} + is \frac{k_y \hat{\mathbf{x}} - k_x \hat{\mathbf{y}}}{k} = \hat{\mathbf{z}} + is \hat{\mathbf{k}}^\perp. \quad (\text{A } 1)$$

Here  $\mathbf{N} = \frac{\mathbf{k} \times \hat{\mathbf{z}}}{|\mathbf{k} \times \hat{\mathbf{z}}|}$  and  $\hat{\mathbf{k}}^\perp = (k_y \hat{\mathbf{x}} - k_x \hat{\mathbf{y}})/k$  are unit vectors orthogonal to the unit vector  $\hat{\mathbf{k}} = \mathbf{k}/k$ . The other two helical modes in the triad are  $\mathbf{h}_s(\mathbf{p}) = \hat{\mathbf{z}} + is \hat{\mathbf{p}}^\perp$  and  $\mathbf{h}_s(\mathbf{q}) = \hat{\mathbf{z}} + is \hat{\mathbf{q}}^\perp$ , where the unit vectors  $\hat{\mathbf{p}}^\perp = (p_y \hat{\mathbf{x}} - p_x \hat{\mathbf{y}})/p$  and  $\hat{\mathbf{q}}^\perp = (q_y \hat{\mathbf{x}} - q_x \hat{\mathbf{y}})/q$  are perpendicular to the unit wave vectors  $\hat{\mathbf{p}} = \mathbf{p}/p$  and  $\hat{\mathbf{q}} = \mathbf{q}/q$ , respectively. The velocity projection onto  $\mathbf{h}_s$  is

$$\begin{aligned} a_s(k_x, k_y, 0, t) &= \frac{\mathbf{h}_s(k_x, k_y, 0) \cdot \hat{\mathbf{u}}(k_x, k_y, 0)}{2} \\ &= \frac{1}{2} [\hat{u}_z(k_x, k_y, 0) + is \left( \frac{\hat{u}_x k_y}{k} - \frac{\hat{u}_y k_x}{k} \right)]. \end{aligned} \quad (\text{A } 2)$$

Since

$$\hat{\omega} = i\mathbf{k} \times \hat{\mathbf{u}} = i(k_x \hat{\mathbf{x}} + k_y \hat{\mathbf{y}}) \times (\hat{u}_x \hat{\mathbf{x}} + \hat{u}_y \hat{\mathbf{y}} + \hat{u}_z \hat{\mathbf{z}}) = i(k_x \hat{u}_y - k_y \hat{u}_x) \hat{\mathbf{z}} = \hat{\omega}_z \hat{\mathbf{z}}, \quad (\text{A } 3)$$

Eq.(A 2) can be also written as

$$a_s(k_x, k_y, 0, t) = \frac{1}{2} \hat{u}_z(k_x, k_y, 0) + \frac{s}{2} \frac{\hat{\omega}_z(k_x, k_y, 0)}{k}. \quad (\text{A } 4)$$

Thus, the vertically-averaged vertical velocity and the vorticity can be separated from the above equation as

$$\hat{u}_z = a_+ + a_-, \quad \hat{\omega}_z = k(a_+ - a_-). \quad (\text{A } 5)$$

For the slow modes  $a_{s_k}(t) = A_{s_k}(t)$ , the ‘‘averaged equation’’ Eq.(2.7) becomes

$$(\partial_t + \frac{1}{Re} k^2) a_{s_k} = \frac{1}{4} \sum_{\mathbf{k}+\mathbf{p}+\mathbf{q}=0} \sum_{s_p, s_q} (s_p p - s_q q) (\mathbf{h}_{s_p}^* \times \mathbf{h}_{s_q}^*) \cdot \mathbf{h}_{s_k}^* a_{s_p}^* a_{s_q}^*. \quad (\text{A } 6)$$

Since  $\hat{\mathbf{p}}^\perp \times \hat{\mathbf{q}}^\perp = \hat{\mathbf{p}} \times \hat{\mathbf{q}}$ ,

$$\begin{aligned} (\mathbf{h}_{s_p}^* \times \mathbf{h}_{s_q}^*) \cdot \mathbf{h}_{s_k}^* &= (\hat{\mathbf{z}} - is \hat{\mathbf{p}}^\perp) \times (\hat{\mathbf{z}} - is \hat{\mathbf{q}}^\perp) \cdot (\hat{\mathbf{z}} - is \hat{\mathbf{k}}^\perp) \\ &= (s_p \hat{\mathbf{p}} - s_q \hat{\mathbf{q}}) \times (s_k \hat{\mathbf{k}} - s_q \hat{\mathbf{q}}) \cdot \hat{\mathbf{z}}. \end{aligned} \quad (\text{A } 7)$$

Then, Eq.(A 6) becomes

$$(\partial_t + \frac{1}{Re} k^2) a_{s_k} = \frac{1}{4} \sum_{\mathbf{k}+\mathbf{p}+\mathbf{q}=0} \sum_{s_p, s_q} (s_p p - s_q q) (s_p \hat{\mathbf{p}} - s_q \hat{\mathbf{q}}) \times (s_k \hat{\mathbf{k}} - s_q \hat{\mathbf{q}}) \cdot \hat{\mathbf{z}}. \quad (\text{A } 8)$$

To construct  $\hat{u}_z$  and  $\hat{\omega}_z$  (Eq.(A 5)) from the above equation, we have

$$\begin{aligned} (\partial_t + \frac{1}{Re} k^2) (a_{+k} - a_{-k}) &= \frac{1}{2} \sum_{\mathbf{k}+\mathbf{p}+\mathbf{q}=0} \frac{p^2 - q^2}{k} (\hat{\mathbf{p}} \times \hat{\mathbf{q}} \cdot \hat{\mathbf{z}}) [-a_{+p}^* a_{+q}^* - a_{-p}^* a_{-q}^* \\ &\quad + a_{+p}^* a_{-q}^* + a_{-p}^* a_{+q}^*], \end{aligned} \quad (\text{A } 9)$$

and

$$\begin{aligned} (\partial_t + \frac{1}{Re} k^2) (a_{+k} + a_{-k}) &= \frac{1}{2} \sum_{\mathbf{k}+\mathbf{p}+\mathbf{q}=0} (\hat{\mathbf{p}} \times \hat{\mathbf{q}} \cdot \hat{\mathbf{z}}) [(p - q) (-a_{+p}^* a_{+q}^* + a_{-p}^* a_{-q}^*) \\ &\quad + (p + q) (a_{+p}^* a_{-q}^* - a_{-p}^* a_{+q}^*)]. \end{aligned} \quad (\text{A } 10)$$

Let  $b_k = a_{+k} - a_{-k}$  and  $\theta_k = a_{+k} + a_{-k}$ , then  $a_{+k} = (\theta_k + b_k)/2$  and  $a_{-k} = (\theta_k - b_k)/2$ . Substituting the above relations into Eq.(A 9) and Eq.(A 10), we have

$$(\partial_t + \frac{1}{Re} k^2) b_k = -\frac{1}{2} \sum_{\mathbf{k}+\mathbf{p}+\mathbf{q}=0} \frac{p^2 - q^2}{k} \hat{\mathbf{p}} \times \hat{\mathbf{q}} \cdot \hat{\mathbf{z}} b_p^* b_q^*, \quad (\text{A } 11)$$

and

$$(\partial_t + \frac{1}{Re} k^2) \theta_k = \frac{1}{2} \sum_{\mathbf{k}+\mathbf{p}+\mathbf{q}=0} \frac{\hat{\mathbf{p}} \times \hat{\mathbf{q}} \cdot \hat{\mathbf{z}}}{pq} [q b_p^* \theta_q^* - p b_q^* \theta_p^*]. \quad (\text{A } 12)$$

Since  $\hat{\omega}_z = k b_k$  from Eq.(A 5), Eq.(A 11) can be written in terms of the vorticity as

$$(\partial_t + \frac{1}{Re} k^2) \hat{\omega}_z = \frac{1}{2} \sum_{\mathbf{k}+\mathbf{p}+\mathbf{q}=0} \frac{\hat{\mathbf{p}} \times \hat{\mathbf{q}} \cdot \hat{\mathbf{z}}}{pq} [q b_p^* \hat{\omega}_{z_q}^* - p b_q^* \hat{\omega}_{z_p}^*]. \quad (\text{A } 13)$$

This is exactly the same as the helical formulation of 2D N-S equation which is given by Waleffe (1993).

Also because of  $\hat{u}_z(\mathbf{k}) = \theta_k$  from Eq.(A 5), Eq.(A 12) can be written in terms of  $\hat{u}_z(\mathbf{k})$  as

$$(\partial_t + \frac{1}{Re} k^2) \hat{u}_{z_k} = \frac{1}{2} \sum_{\mathbf{k}+\mathbf{p}+\mathbf{q}=0} \frac{(\hat{\mathbf{p}} \times \hat{\mathbf{q}} \cdot \hat{\mathbf{z}})}{pq} (q b_p^* \hat{u}_{z_q}^* - p b_q^* \hat{u}_{z_p}^*). \quad (\text{A } 14)$$

This equation has the same structure as the 2D vorticity equation Eq.(A 13). It is known that a 2D passive scalar and the 2D vorticity obey homologous equations and, in fact, the above equation is the helical formulation of the 2D passive scalar equation.

Based on the above discussion, we now summarize the Dynamic Taylor-Proudman theorem as the following: in three-dimensional rotating turbulence, when  $Ro \rightarrow 0$ , “slow-slow-slow” triadic interactions yield the 2D-3C Navier-Stokes equations. Here, 2D-3C refers to two variables  $(x, y)$  and three components  $(\bar{u}^{3D}, \bar{v}^{3D}, \bar{w}^{3D})$ . The vertically-averaged horizontal velocity  $(\bar{u}^{3D}, \bar{v}^{3D}) = \frac{1}{H} \int_0^H (u_x(x, y, z), u_y(x, y, z)) dz$  satisfies the 2D Navier-Stokes equation

$$\partial_t \hat{\omega}_z + \nu k^2 \hat{\omega}_z = -i k_x \bar{u}^{3D}(x, y) \hat{\omega}_z(x, y) - i k_y \bar{v}^{3D}(x, y) \hat{\omega}_z(x, y), \quad (\text{A } 15)$$

and the vertically-averaged vertical velocity  $\bar{w}^{3D} = \frac{1}{H} \int_0^H u_z(x, y, z) dz$  obeys the 2D passive scalar equation

$$\partial_t \widehat{\bar{w}^{3D}}(\mathbf{k}) + \nu k^2 \widehat{\bar{w}^{3D}}(\mathbf{k}) = -i k_x \bar{u}^{3D}(x, y) \widehat{\bar{w}^{3D}}(x, y) - i k_y \bar{v}^{3D}(x, y) \widehat{\bar{w}^{3D}}(x, y). \quad (\text{A } 16)$$

Here,  $H$  is the vertical height of the domain and the three averaged velocity components in the Fourier space are as follows:

$$\widehat{\bar{u}^{3D}}(\mathbf{k}) = i \frac{k_y}{k_x^2 + k_y^2} \hat{\omega}_z(\mathbf{k}), \quad \widehat{\bar{v}^{3D}}(\mathbf{k}) = -i \frac{k_x}{k_x^2 + k_y^2} \hat{\omega}_z(\mathbf{k}), \quad \widehat{\bar{w}^{3D}}(\mathbf{k}) = \hat{u}_z(\mathbf{k}). \quad (\text{A } 17)$$

## REFERENCES

- BABIN, A., MAHALOV, A. & NICOLAENKO, B. 1996 Global splitting, integrability and regularity of 3D Euler and Navier-Stokes equations for uniformly rotating fluids. *Eur. J. Mech. B/Fluids* **15**, 291-300.
- BARDINA, J., FERZIGER, J. H. & ROGALLO, R. S. 1985 Effect of rotation on isotropic turbulence: Computation and modeling. *J. Fluid Mech.* **154**, 321-336.
- BARTELO, P. 1995 Geostrophic adjustment and inverse cascade in rotating stratified turbulence. *J. Atmosph. Sci.* **52**, 4410-4428.

- BARTELLO, P., MÈTAIS, O. & LESIEUR, M. 1994 Coherent structures in rotating three-dimensional turbulence. *J. Fluid Mech.* **273**, 1–29.
- CAMBON, C. & JACQUIN, L. 1989 Spectral approach to non-isotropic turbulence subjected to rotation. *J. Fluid Mech.* **202**, 295–317.
- CELANI, A., LANOTTE, A., MAZZINO, A. & VERGASSOLA, M. 2000 Universality and saturation of intermittency in passive scalar turbulence. *Phys. Rev. Lett.* **84**, 2385–2388.
- CRAIK, A. D. D. 1985 *Wave Interactions and Fluid Flow*. Cambridge University Press.
- EMBED, P. F. & MAJDA, A. J. 1996 Averaging over fast gravity waves for geophysics flows with arbitrary potential vorticity. *Commun. Partial Diff. Eqns.* **21**, 619–658.
- EMBED, P. F. & MAJDA, A. J. 1998 Low Froude number limiting dynamics for stably stratified flow with small or finite Rossby numbers. *Geophys. Astrophys. Fluid Dyn.* **87**, 1–50.
- GREENSPAN, H. P. 1968 *The Theory of Rotating Fluids*. Cambridge University Press.
- GREENSPAN, H. P. 1969 On the nonlinear interaction of inertial waves. *J. Fluid Mech.* **36**, 257–286.
- HOLLOWAY, G. 1979 On the spectral evolution of strongly interactive waves. *Geophys. Astrophys. Fluid Dyn.* **11**, 271–287.
- HOSSAIN, M. 1994 Reduction in the dimensionality of turbulence due to a strong rotation. *Phys. Fluids* **6**, 1077–1080.
- KRAICHNAN, R. H. 1970 Instability in fully developed turbulence. *Phys. Fluids* **13**, 569–575.
- LEITH, C. E. & KRAICHNAN, R. H. 1972 Predictability of turbulent flows. *J. Atmosph. Sci.* **29**, 1041–1058.
- LELONG, P. & RILEY, J. J. 1991 Internal wave-vortical mode interactions in strongly stratified flows. *J. Fluid Mech.* **232**, 1–19.
- LONGUET-HIGGINS, M. S. & GILL, A. E. 1967 Resonant interactions between planetary waves. *Proc. R. Soc. Lond., Ser. A* **299**, 120–140.
- MAHALOV, A., NICOLAENKO B. & ZHOU, Y. 1998 Energy spectra of strongly stratified and rotating turbulence. *Phys. Rev. E* **57**, 6187–6190.
- MAHALOV, A. & ZHOU, Y. 1996 Analytical and phenomenological studies of rotating turbulence. *Phys. Fluids* **8**, 2138–2160.
- MAJDA, A. J. & EMBED, P. F. 1998 Averaging over fast gravity waves for geophysics flows with unbalanced initial data. *Theor. Comp. Fluid Dyn.* **11**, 155–169.
- MANSOUR, N. N., CAMBON, C. & SPEZIALE, C. G. 1992 Theoretical and computational study of rotating isotropic turbulence. In *Studies in Turbulence* (ed. Gatski, T. B., Sarkar, S. & Speziale, C. G). Springer.
- PEDLOSKY, J. 1987 *Geophysical Fluid Dynamics, 2nd Ed.* Springer-Verlag.
- PHILLIPS, O. M. 1960 On the dynamics of unsteady gravity waves of finite amplitude. 1. The elementary interactions *J. Fluid Mech.* **9**, 193–217.
- PHILLIPS, O. M. 1968 The interaction trapping of internal gravity waves. *J. Fluid Mech.* **34**, 407–416.
- PHILLIPS, O. M. 1981 Wave interactions—the evolution of an idea. *J. Fluid Mech.* **106**, 215–227.
- SIGGIA, E. D. & KERR, R. M. 1978 Cascade model of fully developed turbulence. *J. Stat. Phys.* **19**, 543–552.
- SMITH, L. M. & WALEFFE, F. 1999 Transfer of energy to two-dimensional large scales in forced, rotating three-dimensional turbulence. *Phys. Fluids* **6**, 1608–1622.
- SMITH, L. M. & YAKHOT, V. 1993 Bose condensation and small-scale structure generation in a random force driven 2D turbulence. *Phys. Rev. Lett.* **19**, 352–355.
- WALEFFE, F. 1992 The nature of triad interactions in homogeneous turbulence. *Phys. Fluids. A* **4**, 350–363.
- WALEFFE, F. 1993 Inertial transfers in the helical decomposition. *Phys. Fluids. A* **5**, 677–685.
- WARN, T. 1986 Statistical mechanical equilibria of the shallow water equations. *Tellus* **38A**, 1–11.
- YEUNG, P. K. & ZHOU, Y. 1998 Numerical study of rotating turbulence with external forcing. *Phys. Fluids* **10**, 2895–2909.